Electronic supplementary information (ESI)

Functionalization of the Carbon Additive of a High-Voltage Li-Ion Cathode

Hamidreza Saneifar[1], Nicolas Delaporte[1], Karim Zaghib[2*] and Daniel Bélanger[1*]

1. Département de Chimie, Université du Québec à Montréal, Case Postale 8888, succursale Centre-Ville, Montréal (Québec) Canada H3C 3P8.
2. Institut de Recherche d'Hydro-Québec (IREQ), 1800 Boulevard Lionel Boulet, Varennes, Québec, Canada J3X 1S1.

Corresponding author: E-mail: belanger.daniel@uqam.ca E-mail: zaghib.karim@ireq.ca

1. Surface area of LMN and acetylene black (AB).

The BET surface area of the LMN and AB powders was ~ 0.6 and 80 m^2/g [1], respectively. Considering the weight percentages of LMN and AB in the electrode (80 and 10 wt. %, respectively), the surface area of AB exposed to the electrolyte is at least 10 times larger than that of LMN. Thus, it is anticipated that the functionalization of AB will strongly affect processes at the electrolyte/electrode interface and have a strong influence on cell performance.

2. X-ray diffraction

The XRD patterns of modified and unmodified AB carbon powders are presented in Figure S1. This carbon showed three distinguishable diffraction peaks (002), (100) and (110), which indicate a partially graphitic structure. An additional low intensity peak (004) at $2\Theta = 54^{\circ}$ confirms that AB carbon is slightly graphitized, is generally observed for graphite but is more intense [2]. This result confirms that PF_6^- anions could intercalate in the graphitic domains of AB carbon at high voltage, leading to its degradation and poor cycle life of the Li-ion battery [3].

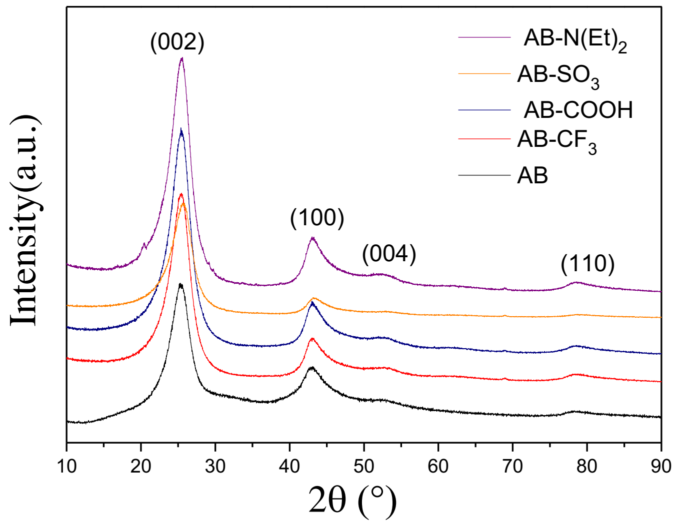

Figure S1. XRD patterns of modified and unmodified AB carbon powders. The patterns are typical of a slightly graphitized carbon.

3. Electrochemical characterization.

Cyclic voltammetry. Figure S2 shows the cyclic voltammogram (2nd cycle) for the aluminum current collector (bare electrode) recorded between: a) 2.5 and 4.8 V and b) 2.5 and 5.3 V vs. Li/Li$^+$. In contrast, the intensity of the current between 4.5 and 5.3 V vs. Li/Li$^+$ is much lower for the carbon electrodes in Figure 2. The charge evaluated for unmodified and modified AB carbons are included in Table S1.

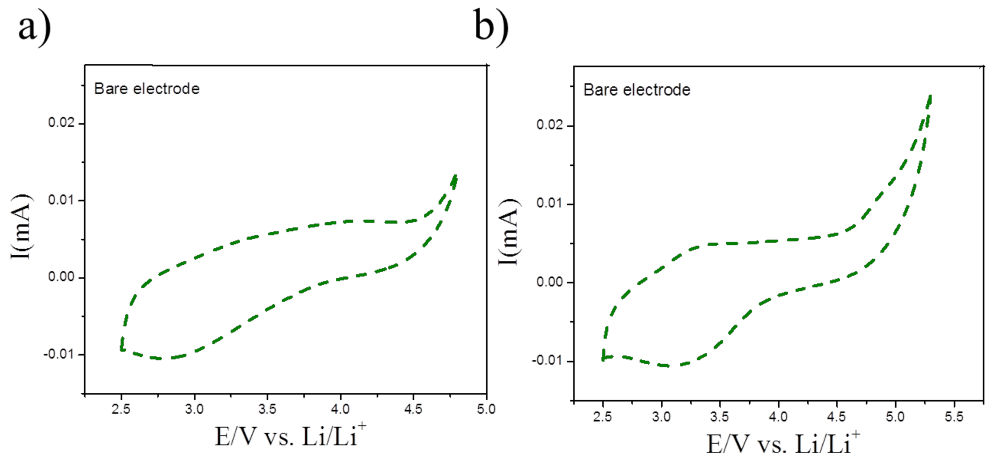

Figure S2. Cyclic voltammograms (2nd cycle) for the aluminum current collector (bare electrode) in 1 M $LiPF_6$ EC:DEC:DMC electrolyte at a scan rate of 10 $mV.s^{-1}$ recorded between: a) 2.5 and 4.8 V and b) 2.5 and 5.3 V vs. Li/Li^+.

Table S1. Q charge and Q discharge (mAh) determined from cyclic voltammograms (2nd cycle) obtained for the Al current collector (bare), unmodified (AB) and modified carbon (AB-X, where X = CF_3, $N(Et)_2$, SO_3H and COOH) electrodes in 1 M $LiPF_6$ EC:DEC:DMC electrolyte at a scan rate of 10 $mV.s^{-1}$ recorded between 2.5 and 4.8 V and 2.5 and 5.3 V vs. Li/Li^+.

	4.8 V		**5.3 V**	
	Q charge (Oxidation) mAh	Q discharge (Reduction) mAh	Q charge (Oxidation) mAh	Q discharge (Reduction) mAh
Al bare	0.00029	0.00026	0.00046	3.25×10^{-7}
AB	0.01334	0.00841	0.24978	0.01238
AB-CF_3	0.00575	0.00576	0.28262	0.06227
AB-COOH	0.01532	0.00552	0.19395	0.01814
AB-SO_3H	0.00634	0.00696	0.20192	0.04389
AB-$N(Et)_2$	0.00698	0.00529	0.17535	0.00896

Galvanostatic cycling of carbon electrodes. Figure S3 presents the charge (Figure S3a) and the discharge (Figure S3b) capacities obtained for unmodified (AB) and modified carbon (AB-X, where X = CF_3, $N(Et)_2$, SO_3H and COOH) electrodes over 10 cycles. The charge capacity of the modified carbon electrodes was one order of magnitude lower, suggesting that electrolyte degradation was considerably reduced. The discharge capacities for all of the carbon electrodes were relatively low and primarily due to the electrical double-layer capacitance[4]. However, the slightly higher discharge capacities obtained for unmodified AB carbon electrode could be due to the intercalation/deintercalation of PF_6^- anions between the graphitic sheets of carbon[5].

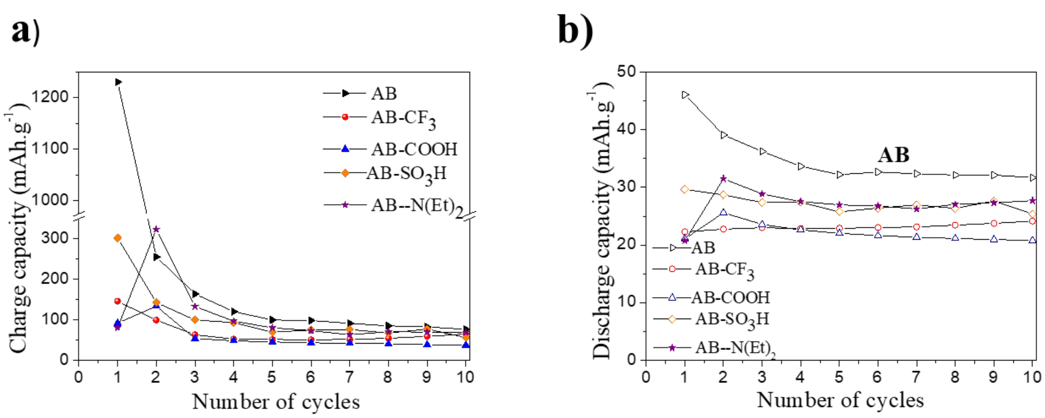

Figure S3. a) Charge and b) discharge capacities (per g of active material) obtained for unmodified (AB) and modified carbon (AB-X, where X = CF_3, $N(Et)_2$, SO_3H and COOH) electrodes cycled with a constant current of 50 $mA.g^{-1}$ between 2.5 and 5.3 V vs. Li/Li^+ for 10 cycles. Note the break (between 300 and 1000 $mAh.g^{-1}$) on the charge capacity axis of the left-hand side figure.

Galvanostatic cycling of LMN electrodes. Table S2 reports the discharge capacity of several half-cells. The electrochemical experiments were repeated three times and the discharge capacities of the LMN half-cells (10^{th} discharge capacity at C/10) are reproducible.

Table S2. Discharge capacities (10^{th} cycle, in $mAh.g^{-1}$) obtained for three different LMN half-cells containing unmodified (LMN-AB) and modified carbons (LMN-AB-X, where X = CF_3, $N(Et)_2$, SO_3H and COOH) and cycled at a rate of C/10 between (top) 3.5 and 5 V and (bottom) 3.5 and 5.3 V vs. Li/Li^+. Average and standard deviation (SD) values are also included.

5 V	**LMN-AB**	**LMN-AB-CF_3**	**LMN-AB-COOH**	**LMN-AB-SO_3H**	**LMN-AB-$N(Et)_2$**
Cell1 ($mAh.g^{-1}$)	86.8	117.7	106.7	116.2	104.1
Cell2 ($mAh.g^{-1}$)	85.1	116.6	105.4	115.4	103.8
Cell3 ($mAh.g^{-1}$)	86.5	115.3	105.9	116.1	104.0
Average ±SD	86.1±0.7	116.5±0.9	106.0±0.5	115.9±0.3	104.0±0.1
5.3 V	**LMN-AB**	**LMN-AB-CF_3**	**LMN-AB-COOH**	**LMN-AB-SO_3H**	**LMN-AB-$N(Et)_2$**
Cell1 ($mAh.g^{-1}$)	88.7	114.3	106.9	121.3	106.2
Cell2 ($mAh.g^{-1}$)	87.1	113.8	105.1	120.8	105.9
Cell3 ($mAh.g^{-1}$)	88.6	114.5	106.7	121.1	106.5
Average±SD	88.1±0.7	114.2±0.3	106.2±0.8	121.1±0.2	106.2±0.2

Comparison of discharge capacities. Table S3 compares discharge capacities obtained for LMN-AB half-cells containing unmodified carbon (LMN-AB) and those extracted from the literature.

Table S3. Discharge capacities of LMN-AB half-cells from our study and the literature.

Capacity (mAh/g)	**Voltage (V)**	**C rate**	**References**
87	3.5-4.9	C/12	6
103	3.5-5	C/10	7
100	3.5-4.85	C/7.5	8
97	3.4-4.9	C/10	9
108	3.5-4.9	C/10	10
127	3.5-5	C/5	11
121	36-4.9	C/10	12
131	3.5-4.9	C/5	13
88	3.5-5	C/10	This work
96	3.5-5.3	C/10	This work

Table S4. Atomic content (at. %) determined from XPS spectra for: a) unmodified (AB), modified carbon electrode (AB-X, with X = $N(Et)_2$ or SO_3H) following cycling at 50 mA/g between 2.5 and 5.3 V for 7 cycles and: b) LMN electrodes with unmodified (LMN-AB) and modified carbons (LMN-AB-X, where X = CF_3 and SO_3H) following cycling at C/10 between 3.5 and 5.3 V for 15 cycles.

a)

AB electrodes		C1s					F1s			P2p				
		C-C	CH_2	C-O	C=O	CF_2	LiF	P-F	PVDF	$Li_xPF_yO_z$	Li_xPF_y			
AB	B.E. (eV)	284.4	286	286.5	288.4	290.7	685.7	687.7	688.8	134.3	135.9			
	FWHM (eV)	1.5	1.5	1.5	1.5	1.5	1.5	1.5	1.5	1.8	1.8			
	Peak area (%)	17.9	29.8	19.6	6.2	26.4	10.1	56.2	33.7	76.9	23			
	Atomic content (at. %)	C1s 47.7					F1s 34.3			P2p 1.9		O1s 15.3	N1s -	S2p -
AB-SO_3H		C1s					F1s			P2p				
		C-C	CH_2	C-O	C=O	CF_2	LiF	P-F	PVDF	$Li_xPF_yO_z$	Li_xPF_y			
	B.E. (eV)	284.5	286.1	286.5	288	290.8	-	687.1	688.3	134.4	135.9			
	FWHM (eV)	1.3	1.3	1.3	1.33	1.3	-	1.7	1.7	2.1	2.1			
	Peak area (%)	50.2	15.6	9	10	15.1	-	25.9	74.1	33.3	66.7			
	Atomic content (at. %)	C1s 61.1					F1s 27.5			P2p 0.5		O1s 9.5	N1s 0.3	S2p 0.4
AB-$N(Et)_2$		C1s					F1s			P2p				
		C-C	CH_2	C-O	C=O	CF_2	LiF	P-F	PVDF	$Li_xPF_yO_z$	Li_xPF_y			
	B.E. (eV)	284.5	286.3	286.8	288.6	291	-	687.2	688.2	134.5	135.6			
	FWHM (eV)	1.1	1.1	1.1	1.1	1.1	-	1.5	1.5	1.5	1.5			
	Peak area (%)	52.8	16.9	10.5	3.6	16.2	-	35.7	64.3	41.7	58.3			
	Atomic content (at. %)	C1s 60.7					F1s 26.1			P2p 0.7		O1s 11.5	N1s 0.3	S2p -

The unmodified and modified acetylene black (AB) carbons were mixed with polyvinylidenedifluoride in a 0.8:1 weight ratio to fabricate the electrodes.

b)

LMN electrodes		C1s					O1s			F1s			P2p					
		C-C	CH_2	C-O	C=O	CF_2	C-O	C=O	M-O	LiF	P-F	PVDF	$Li_xPF_yO_z$	Li_xPF_y				
LMN-AB	B.E. (eV)	284.6	286.2	286.6	288.2	290.6	533	531.6	529.6	685.5	687.3	688.3	134.2	135.9				
	FWHM (eV)	1.6	1.6	1.6	1.6	1.6	2	2	2	1.2	1.8	1.8	1.9	1.9				
	Peak area (%)	24.3	24.3	19.4	9.7	22.2	37.1	59.5	3.3	9.3	54.3	36.1	43.4	56.5				
	Atomic content (at. %)	C1s 56					O1s 17.2			F1s 25.5			P2p 0.8		N1s -	S2p -	Mn2p 0.4	Ni2p <0.1
LMN-AB-SO_3H		C1s					O1s			F1s			P2p					
		C-C	CH_2	C-O	C=O	CF_2	C-O	C=O	M-O	LiF	P-F	PVDF	$Li_xPF_yO_z$	Li_xPF_y				
	B.E. (eV)	284.7	286.2	286.5	288.1	290.7	533.3	531.9	529.8	-	687.4	688.3	134.3	136.2				
	FWHM (eV)	1.3	1.3	1.3	1.3	1.3	2.1	2.1	2.1	-	1.6	1.6	2.1	2.1				
	Peak area (%)	43.4	21.7	9.5	5.22	20	31.2	56.2	12.5	-	37.4	62.5	35.7	64.3				
	Atomic content (at. %)	C1s 53.4					O1s 18.7			F1s 22.4			P2p 1.1		N1s 0.2	S2p <0.1	Mn2p 2	Ni2p 0.3
LMN-AB-CF_3		C1s					O1s			F1s			P2p					
		C-C	CH_2	C-O	C=O	CF_2	C-O	C=O	M-O	LiF	P-F	PVDF	$Li_xPF_yO_z$	Li_xPF_y				
	B.E. (eV)	284.6	286	286.3	288.1	290.4	533	531.6	529.3	-	687.3	688.2	134.2	136.2				
	FWHM (eV)	1.3	1.3	1.3	1.3	1.3	2.2	2.2	2.2	-	1.4	1.8	1.8	1.8				
	Peak area (%)	49.9	17.4	10	15	7.5	38.5	53.8	7.7	-	33.3	66.7	62.5	37.5				
	Atomic content (at. %)	C1s 62.1					O1s 10.1			F1s 25.7			P2p 0.7		N1s -	S2p -	Mn2p 0.9	Ni2p <0.1

The $LiMn_{1.5}Ni_{0.5}O_4$ (LMN) powder was mixed with unmodified and modified acetylene black (AB) carbon and polyvinylidenedifluoride (PVDF) in a weight ratio of 80:10:10

References

1 A. Gambou-Bosca, D. Bélanger, J. Mater. Chem. A, 2014, **2,** 6463-6473.

2 Z.Q. Li, C.J. Lu, Z.P. Xia, Y. Zhou, Z. Luo, Carbon N. Y, 2007, **45,** 1686–1695.

3 X. Qi, B. Blizanac, A. Dupasquier, P. Meister, T. Placke, M. Oljaca, J. Li, M. Winter, Phys. Chem. Chem. Phys, 2014, **16,** 25306–25313.

4 A.J. Chmiola, G. Yushin, Y. Gogotsi, C. Portet, P. Simon, P.L. Taberna, Science, 2015, **313,** 1760–1763.

5 T. Ishihara, M. Koga, H. Matsumoto, M. Yoshio, Electrochem. Solid-State Lett, 2007, **10,** A74–A76.

6 H. Duncan, D. Duguay, Y. Abu-Lebdeh, I.J. Davidson, J. Electrochem. Soc, 2011,**158,** A537–A545.

7 C.J. Jafta, M.K. Mathe, N. Manyala, W.D. Roos, K.I. Ozoemena, ACS Appl. Mater. Interfaces, 2013, **5,** 7592–7598.

8 H.-M. Cho, M.V. Chen, A.C. MacRae, Y.S. Meng, ACS Appl. Mater. Interfaces, 2015, **7,** 16231–16239.

9 F. Ulu Okudur, J. D'Haen, T. Vranken, D. De Sloovere, M. Verheijen, O.M. Karakulina, A.M. Abakumov, J. Hadermann, M.K. Van Bael, A. Hardy, RSC Adv, 2018, **8,** 7287–7300.

10 Q. Wu, Y. Yin, S. Sun, X. Zhang, N. Wan, Y. Bai, Electrochim. Acta. 2015, **158,** 73–80.

11 D. Liu, Y. Bai, S. Zhao, W. Zhang, J. Power Sources. 2012, **219,** 333–338.

12 H. Dong, G.M. Koenig, J. Mater. Chem. A. 2017, **5,** 13785–13798.

13 P. Axmann, G. Gabrielli, M. Wohlfahrt-Mehrens, J. Power Sources. 2016, **301,** 151–159.